Eur Biophys J (1991) 20:183–191

European Biophysics Journal

The interactions of horse heart apocytochrome *c* with phospholipid vesicles and surfactant micelles: time-resolved fluorescence study of the single tryptophan residue (*Trp-59*)

M. Vincent and J. Gallay

Laboratoire pour l'Utilisation du Rayonnement Electromagnétique, Centre National de la Recherche Scientifique, Ministère de l'Education Nationale et de la Jeunesse et des Sports, Commissariat à l'Energie Atomique, Université Paris Sud, Bâtiment 209D, F-91405 Orsay Cedex, France

Received January 28, 1991/Accepted in revised form June 7, 1991

Abstract. The interactions of horse heart apocytochrome *c* with membrane interfaces were studied on membrane models including micelles of the anionic surfactant sodium dodecyl sulfate (SDS), the micelle forming lipid analogs dodecylphosphoglycol (C12PG), tetradecylphosphoglycol (C14PG), and dodecylphosphocholine (C12PN), and the negatively charged phospholipid 1-palmitoyl-2-oleoyl-sn-glycero phosphocholine (POPS) forming small unilamellar vesicles (SUV). The time-resolved fluorescence of the single tryptophan residue (*Trp-59*) emission was monitored to characterize the modifications of the conformational equilibrium and of the internal dynamics of the protein, which can be brought about by its binding to these model membranes. In most of the cases, as for the protein in solution, the excited state lifetime distribution of the Trp emission was described by four discrete classes, whose relative proportions and barycenters vary significantly in the different complexes formed. In the complex with POPS, however, the decay analysis showed only 3 lifetime classes: the long lifetime class displayed a barycenter value smaller than that observed for the protein in aqueous solution but with a much higher proportion, indicating a stabilization of this conformer in the membrane-bound form of the protein. A similar sensitivity of the *Trp-59* excited state to deactivation by thermal collisions in water and in the protein/POPS complex was observed, indicating a probable location of *Trp-59* at the membrane/water interface. The effects of protein binding to C12PN, C12PG and C14PG micelles on the long lifetime class proportion were similar to that of POPS but, in addition, there was a large contribution of a short lifetime component which was absent in POPS vesicles. The barycenter values of the excited state lifetime classes were comparable in these membrane systems, suggesting that *Trp-59* is not transferred to a non-polar environment. Binding of apocytochrome *c* to SDS micelles strongly reduced the lifetime class barycenters and, in contrast to the other membrane systems, strongly favored the contribution of the shortest lifetime class at the expense of the c_3 class. This suggests an interaction of the *Trp-59* with the sulfur containing head-group of this surfactant. The indole ring mobility is reduced at the interface contacts. A fast *Trp-59* mobility with a large amplitude is suggested in the complex with POPS by an initial anisotropy value lower than the expected one of 0.295 measured in vitrified medium. These observations can be correlated with the induction of α-helical structure after interactions of apocytochrome *c* with membrane model systems (de Jongh and de Kruijff 1990).

Key words: Apocytochrome *c* – Tryptophan – Time-resolved fluorescence

Abbreviations: AOT, sodium bis-(2-ethylhexyl)sulfosuccinate; C12PG, dodecylphosphoglycol; C14PG, tetradecylphosphoglycol; C12PN, dodecylphosphocholine; MEM, Maximum Entropy Method; NMR, nuclear magnetic resonance; POPS, 1-palmitoyl, 2-oleoyl-sn-glycerophosphoserine; SUV, small unilamellar vesicles; *Trp*, tryptophan

Offprint requests to: J. Gallay

Introduction

The intrinsic flexible nature of apocytochrome *c* – a single tryptophan containing protein – in aqueous solution was demonstrated by a recent time-resolved fluorescence study (Vincent et al. 1988). Despite this wide flexibility, both the excited state lifetime and the rotational correlation time distributions suggested the existence of defined conformers slow to exchange in the nanosecond time scale. After a two-dimensional analysis by MEM, a correlation between the fastest flexibility and the excited state population displaying the shortest excited state lifetime was suggested (Brochon and Livesey 1987). Such a flexibility is expected to be of great importance for the accommodation of the apoprotein to changing environments during the translocation from the cytoplasmic compartment where it is synthesized to the mitochondrion where the heme group is enzymatically bound (Hennig et al., 1983). Changes in the *Trp-59* environment and in the overall protein structure have already been observed by steady-state fluorescence, CD and NMR measure-

ments upon interaction of apocytochrome *c* with membrane models constituted with negatively charged lipids (Rietveld et al. 1985; Berkhout et al. 1987; de Jongh and de Kruijff 1990). It was therefore interesting to compare the dynamic behavior of this protein after binding to membrane interfaces with that in solution. A time-resolved fluorescence study of the interactions of horse heart apocytochrome *c* with membrane interfaces was therefore undertaken. Membrane models including the anionic surfactant SDS, the micelle forming lipid analogs alkyl phosphoglycols or alkyl phosphocholine, and POPS SUV, were used to specify the modifications of the local conformational equilibrium and internal dynamics of the protein, brought about by its binding to these model membranes.

Materials and methods

Chemicals

Apocytochrome *c*, C12PN, C12PG and C14PG were generous gifts from W. Jordi and H. de Jongh in Prof. B. de Kruijff's laboratory (University of Utrecht, The Netherlands). SDS was purchased from Merck (Darmstadt, RFA). POPS was from Avanti Polar Lipids (Birmingham, Ala) and was used as supplied. POPS SUV were prepared by sonication using a probe sonifier. The protein/lipid ratio was ~1/20. Dimethyl glutaric acid (Merck, Darmstadt) was used as buffer at pH 7.

Fluorescence measurements

Total fluorescence and anisotropy decays were obtained from the polarized components $I_{vv}(t)$ and $I_{vh}(t)$ on the experimental set-up installed on the SB1 window of the synchrotron radiation machine Super-ACO (Anneau de Collision d'Orsay) which has been described elsewhere (Kuipers et al. 1990). The storage ring provides a light pulse with a full width at half maximum (FWHM) of ~500 ps at a frequency of 8.33 MHz for a double bunch mode. The excitation wavelength was set at 300 nm (bandwidth 5 nm). The emission wavelength was set at 350 nm (bandwidth 10 nm). A Hamamatsu microchannel plate R1564U-06 was utilized. Data for $I_{vv}(t)$ and $I_{vh}(t)$ were stored in separate memories of a plug-in multichannel analyzer card (Canberra) in a DESKPRO 286E microcomputer (Compaq). Accumulations were stopped when $\sim 10^5$ counts were stored in the peak channel for the total fluorescence intensity decay. Time resolution was routinely ~30 ps per channel and 1024 channels were used. The instrumental response function was automatically monitored in alternation with the parallel and perpendicular components of the polarized fluorescence decay by measuring the sample scattering light at the emission wavelength. The automatic sampling of the data was driven by the microcomputer.

Data analysis

Data analysis of the total intensity decay was performed by the Maximum Entropy Method (Livesey and Brochon 1987) using MEMSYS2 as a subroutine library (MEDC, Ltd).

The principles of MEM as applied to time-resolved fluorescence are outlined in the following. With vertically polarized light, the parallel $I_{vv}(t)$ and perpendicular $I_{vh}(t)$ components of the fluorescence intensity at time t after the start of the excitation are:

$$I_{vv}(t) = \tfrac{1}{3} E_\lambda(t) * \int_0^\infty \int_0^\infty \int_{-0.2}^{0.4} \gamma(\tau, \theta, A) \cdot e^{-t/\tau}(1 + 2A\, e^{-t/\theta})\, d\tau\, d\theta\, dA \quad (1)$$

and

$$I_{vh}(t) = \tfrac{1}{3} E_\lambda(t) * \int_0^\infty \int_0^\infty \int_{-0.2}^{0.4} \gamma(\tau, \theta, A) \cdot e^{-t/\tau}(1 - A\, e^{-t/\theta})\, d\tau\, d\theta\, dA \quad (2)$$

where $E_\lambda(t)$ is the temporal shape of the excitation flash, * denotes a convolution product and $\gamma(\tau, \theta, A)$ represents the number of fluorophores with fluorescence lifetime τ, rotational correlation time θ and initial anisotropy A.

If we are only interested in the determination of the total intensity decay parameters, we can considerably simplify the analysis by summing the parallel and perpendicular components:

$$T(t) = I_{vv}(t) + 2\, I_{vh}(t) = E_\lambda(t) * \int_0^\infty \alpha(\tau)\, e^{-1/\tau}\, d\tau \quad (3)$$

$\alpha(\tau)$ is the lifetime distribution given by:

$$\alpha(\tau) = \int_0^\infty \int_{-0.2}^{0.4} \gamma(\tau, \theta, A)\, d\theta\, dA\,. \quad (4)$$

In order to ensure our recovered distribution agrees with our data, we maximize S:

$$S = \int_0^\infty \alpha(\tau) - m(\tau) - \alpha(\tau) \log \frac{\alpha(\tau)}{m(\tau)} d\tau \quad (5)$$

where $m(\tau)$ is the starting lifetime distribution flat in $\log \tau$ space and $\alpha(\tau)$ is the resulting distribution.

S was subjected to the following constraint:

$$\sum_{k=1}^{M} \frac{(T_k^{\text{calc}} - T_k^{\text{obs}})^2}{\sigma_k^2} \leq M \quad (6)$$

where T_k^{calc} and T_k^{obs} are the k^{th} calculated and observed intensities. σ_k^2 is the variance of the k^{th} point ($\sigma_k^2 = \sigma_{k,vv}^2 + 4\,\beta_{\text{corr}}^2\,\sigma_{k,vh}^2$, Wahl (1979). M is the total number of observations and β_{corr} is a factor compensating for the difference in transmission by the emission monochromator of the parallel and perpendicular light.

The center τ_j of lifetimes over the $\alpha(\tau_i)$ distribution is defined as:

$$\tau_j = \sum_i \alpha(\tau_i)\, \tau_i / \sum_i \alpha(\tau_i) \quad (7)$$

the summation being performed on the significant values of the $\alpha_i(\tau_i)$ for the j class. C_i is the normalized contribution of the lifetime class j. A lifetime domain spanning 150 values, equally spaced on a logarithmic scale between 0.1 and 20.0 ns, was routinely used in the analyses.

Fluorescence anisotropy decay

In the analysis of the data as in Karplus's formalism (Ichiye and Karplus 1983), all the emitting species are assumed to display the same intrinsic anisotropy and rotational dynamics. If such were the case Eqs. (1) and (2) can be rewritten as:

$$I_{vv}(t) = \tfrac{1}{3} E_\lambda(t) * \int_0^\infty \alpha(\tau)\, e^{-t/\tau}\, d\tau \left[1 + 2\int_0^\infty \beta(\theta)\, e^{-t/\theta}\, d\theta\right] \quad (8)$$

and

$$I_{vh}(t) = \tfrac{1}{3} E_\lambda(t) * \int_0^\infty \alpha(\tau)\, e^{-t/\tau}\, d\tau \left[1 - \int_0^\infty \beta(\theta)\, e^{-t/\vartheta}\, d\theta\right] \quad (9)$$

with

$$A_0 = \int_0^\infty \beta(\theta)\, d\theta \quad (10)$$

where $\beta(\theta)$ is the rotational correlation time distribution and the other symbols have the same meaning as in (1). The $\alpha(\tau)$ profile is given from a first analysis of $T(t)$ by MEM and is held constant in a subsequent and global analysis of $I_{vv}(t)$ and $I_{vh}(t)$ which provides the distribution $\beta(\theta)$ of correlation times (Brochon and Livesey 1991). 100 rotational correlation time values, equally spaced in logarithmic scale and ranging from 0.01 to 50 ns were used for the analysis of $\beta(\theta)$.

The barycenters of the correlation time distribution are calculated as:

$$\theta_j = \frac{\sum_j \beta_i(\theta_i)\,\theta_i}{\sum_i \beta_i(\theta_i)} \quad (11)$$

β_i is the contribution of the rotational correlation time i to the class j.

Interpretation of the data

Following the Karplus formalism (Ichiye and Karplus 1983), if the fast rotational motion decays exponentially with a relaxation time θ and reaches a plateau value P_∞, we have:

$$A(t) = A_0\,[(1 - P_\infty)\exp(-t/\theta) + P_\infty]\exp(-t/\theta_m) \quad (12)$$

where θ_m is the overall rotational correlation time of the protein.

If the fast rotational motion corresponds to a correlation function that separates into two time scales (θ_1 and θ_2), the expression of the anisotropy can be written as:

$$A(t) = A_0\,\{[(1 - P_{\infty,1})\exp(-t/\theta_1) + P_{\infty,1}][(1 - P_{\infty,2}) \cdot \exp(-t/\theta_2) + P_{\infty,2}]\}\exp(-t/\theta_m) \quad (13)$$

with $\theta_1 \ll \theta_2 \ll \theta_m$. $P_{\infty,i}$ are the plateau values of the correlation function describing these internal motions. A_0 is the intrinsic anisotropy measured in the absence of any rotational motion, related to the angle α between the absorption and emission dipoles:

$$A_0 = \frac{2}{5}\left[\frac{(3\cos^2\alpha - 1)}{2}\right]. \quad (14)$$

The above expression of the anisotropy decay can be rewritten as:

$$A(t) = \beta_1 \exp(-t/\theta_1) + \beta_2 \exp(-t/\theta_2) + \beta_3 \exp(-t/\theta_m) \quad (15)$$

if $\beta_1 = (1 - P_{\infty,1})\,A_0$, $\beta_2 = P_{\infty,1}(1 - P_{\infty,2})\,A_0$ and $\beta_3 = P_{\infty,1} \times P_{\infty,2}\,A_0$.

In principle, if the resolution of the experiment is such that it allows the description of all the rotational motions, the initial effective value of the anisotropy ($A_{0\,\mathrm{eff}} = \sum \beta_j$) must be equal to the A_0 value measured in the absence of motion ($A_0 = 0.295$ at 300 nm in glycerol at -38 °C; Vincent et al. 1988). If short rotations cannot be resolved, the extrapolated $A_{0\,\mathrm{eff}}$ value can be different from the A_0 value. If it is assumed that the A_0 value remains unchanged in the different membrane systems, *the order parameter* (S_1) *associated to the subnanosecond motion of the indole ring* can be indirectly calculated using the $A_{0\,\mathrm{eff}}$ and the A_0 values, as described by Levy and Szabo (1982).

The cone semiangle ($\omega_{\max}$) of the *subnanosecond rotation* of the fluorophore transition dipole (Kinosita et al. 1977; Lipari and Szabo 1980) and the associated orientational order parameter (S_1) can be calculated from:

$$(\beta_2 + \beta_3)/A_0 = S_1^2 = [\cos\omega_{\max}(1 + \cos\omega_{\max})/2]^2. \quad (16)$$

The application of such a model to the *Trp* motion inside a protein is only for the sake of comparison, since the geometry of the motion remains unknown.

The overall correlation of the rotating particle as a whole can be described simply in an equivalent sphere approximation model as:

$$\theta_m = V_h\,\eta/k\,T \quad (17)$$

where V_h is the hydrated volume of the particle, η the solvent viscosity and T the temperature. From the correlation time value, the hydrated volume and the Stokes radius values can be calculated.

Results

Excited state lifetime distribution of Trp-59 in apocytochrome c

As found at pH 5, the total fluorescence intensity decay of *Trp-59* of apocytochrome *c* is described at pH 7 by MEM analysis as resulting from the emission of four classes of excited state (Fig. 1). The fluorescence decay parameters are very similar to those previously found under the former pH conditions (Vincent et al. 1988). One can observe, as in other peptides or proteins possessing a *Trp* residue exposed to the solvent (see for examples John and Jähnig 1988; Vincent et al. 1988; Kuipers et al. 1990), lifetime classes with barycenters ~ 0.5 and ~ 3 ns, which are also present for *Trp* in buffer solution at pH 7 (Szabo and Rayner 1980; Chang et al. 1983; Petrich et al. 1983; Creed 1984) and which therefore may arise from similar kinds of interactions in the excited state as those assumed for *Trp* in solution (Table 1). In addition to these lifetime classes others are frequently detected in *Trp* fluorescence decays in proteins and can be attributed to

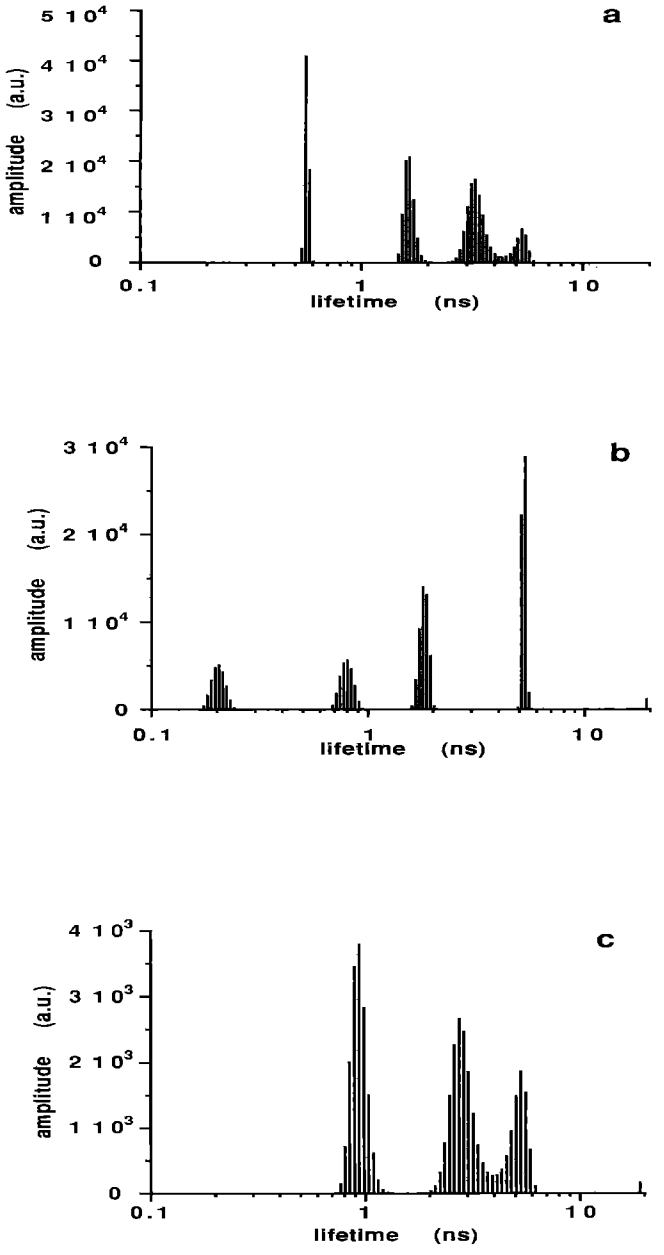

Fig. 1a–c. MEM recovered spectra of *Trp-59* excited state lifetime distribution of apocytochrome *c* in solution (**a**) and in interaction with C12PN micelles (**b**) and POPS sonicated vesicles (**c**). Experimental conditions were: protein concentration 20 μM, temperature: 20 °C, excitation wavelength: 300 nm, emission wavelength: 350 nm

specific interactions with amino acid groups surrounding the *Trp* residue.

The interaction of the apocytochrome *c* protein with all the membrane model systems leads to large modifications of the excited state lifetime distribution. Mainly, in the complex of the protein with SDS, the relative concentration of the shortest excited state lifetime population is increased at the expense of the c_3 class. A stronger quenching environment is also provided by the SDS micelles since a reduction of the barycenter values for each lifetime class is observed. This is mainly so for c_1 and c_2 classes. The presence of a sulfur atom seems to generate the occurrence of short lifetime species in high proportions (Table 1).

For the cases of the alkyl phospocholine (C12PN) (Fig. 1) and alkyl phosphoglycerol (C12 and C14PG), even larger modifications of the lifetime distributions are detected (Table 1). With all these surfactants, the contribution of the longest class of excited state lifetimes is strongly increased. The maximum effect is observed for C12PN: the relative proportion of the long component is increased by factor 4.25 (Fig. 1 and Table 1). This increase occurs mainly at the expense of the c_3 class. In the case of C12 and C14PG, the c_4 class is increased by only factors of 2 and 2.25 respectively (Table 1). For all these surfactant apocytochrome *c* complexes, the barycenter value of each lifetime class is strongly decreased, indicating that non-radiative processes are more efficient in these complexes as compared to apocytochrome *c* in water solutions.

In the apocytochrome *c* complex with POPS (protein/phospholipid ratio ~ 120), the situation is somewhat different. An extremely short excited state lifetime (20 ps) was detected in the analysis (data not shown), but we have considered that it bore no physical significance owing to the large scattering of the sample and to the time resolution of the measurements (32 ps). Therefore, the main effect of apocytochrome *c* binding to POPS is that the shortest excited state lifetime class disappears to the benefit of the longest one (Fig. 1 and Table 1).

As a function of temperature, the excited state lifetime values are decreased. In buffer, the minor long lifetime τ_4 value is decreased by 25% in the temperature range studied, τ_2 and τ_3 values are decreased by 39 and 52% respectively. τ_1 is not affected (Fig. 2). No change in the relative amplitudes are observed (Fig. 3). In POPS vesicles, the

Table 1. Total intensity decay parameters of *Trp-59* in horse heart apocytochrome *c* in aqueous solution and in interaction with surfactant micelles and POPS SUV. Apocytochrome *c* concentration: 20 μM in 0.01 M sodium phosphate buffer pH 7.04. Temperature: 20 °C. Excitation wavelength: 300 nm (band width: 5 nm). Emission wavelength: 350 nm (band width: 10 nm). Data analyses were performed with MEM as a sum of exponentials (Livesey and Brochon, 1987)

Sample	c_1	c_2	c_3	c_4	$\tau_{1(ns)}$	$\tau_{2(ns)}$	$\tau_{3(ns)}$	$\tau_{4(ns)}$	$\langle\tau\rangle_{(ns)}$
Buffer	0.26±0.01	0.29±0.01	0.38±0.03	0.08±0.03	0.56±0.01	1.66±0.01	3.43±0.14	5.67±0.46	2.38
SDS (0.5%)	0.43±0.04	0.30±0.05	0.20±0.01	0.07±0.01	0.30±0.11	0.97±0.17	2.28±0.02	4.33±0.13	1.18
C12PN (0.1%)	0.20±0.04	0.20±0.03	0.27±0.04	0.34±0.01	0.16±0.04	0.85±0.05	1.93±0.12	5.22±0.01	2.50
C12PG (0.1%)	0.23±0.04	0.36±0.04	0.25±0.02	0.16±0.01	0.18±0.01	0.91±0.06	2.25±0.21	4.31±0.10	1.62
C14PG (0.1%)	0.32	0.31	0.19	0.18	0.20	1.02	2.11	4.09	1.52
POPS	–	0.36±0.02	0.39±0.02	0.24±0.04	–	0.82±0.12	2.53±0.17	4.90±0.23	2.46

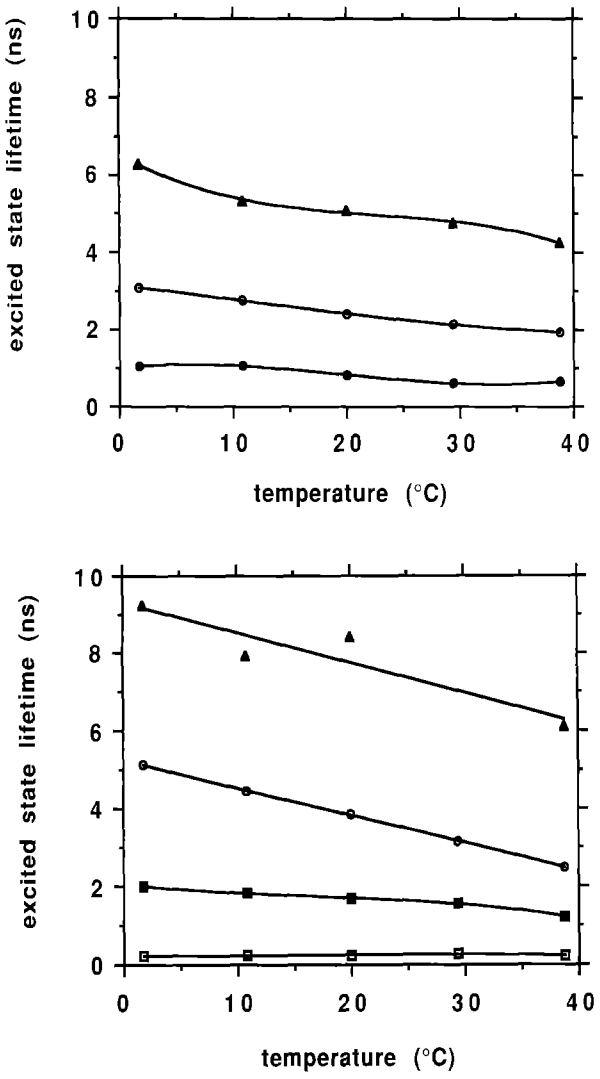

Fig. 2. Variation as a function of temperature of the barycenter values of the *Trp-59* excited state lifetime classes for apocytochrome *c* in buffer solution pH 7 (*lower panel*) and in interaction with POPS sonicated vesicles (*upper panel*)

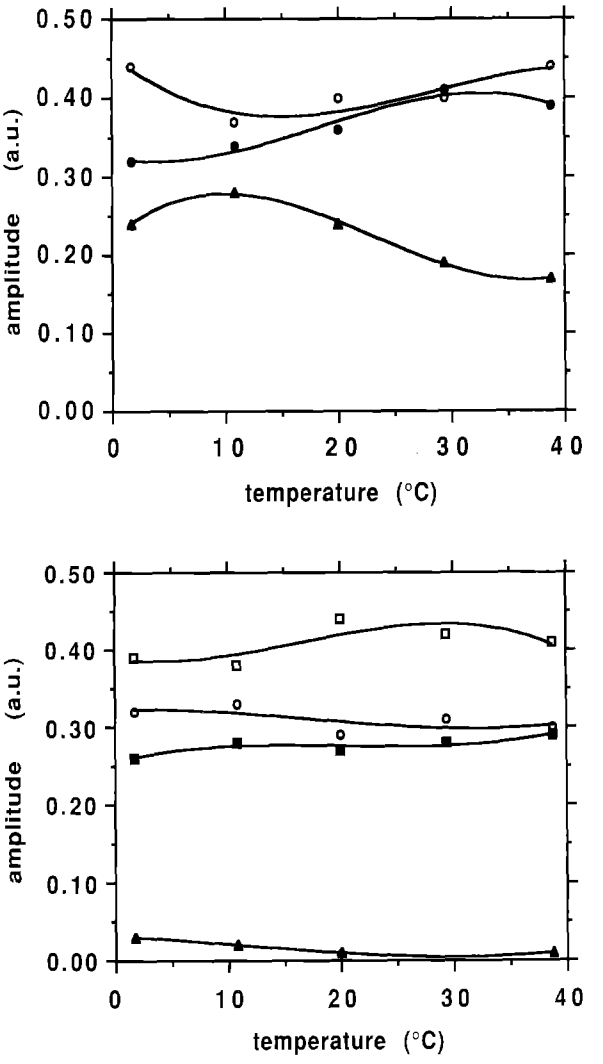

Fig. 3. Variation as a function of temperature of the relative amplitudes of the *Trp-59* excited state lifetime classes of apocytochrome *c* in buffer solution pH 7 (*lower panel*) and in interaction with POPS sonicated vesicles (*upper panel*)

decreases of the excited state lifetime values are 37, 32 and 41% respectively (Fig. 2) and a change in the proportions of the excited state lifetime populations occurs (Fig. 3).

Mobility of the Trp-59 residue in apocytochrome c in solution and in the complexes

The fluorescence anisotropy decay measurements provide information about the rotational dynamics of the *Trp* residue and about the overall rotation of the whole particle on which the protein is bound. An example of an anisotropy decay and of its analysis by MEM is provided in Figs. 4 and 5, respectively. In aqueous solution, as at pH 5 (Vincent et al. 1988), the apocytochrome *c* protein appears to be dimeric according to the value of the longest correlation time (Table 2). Two internal motions, characterized by short correlation times (θ_1 and θ_2) differing by almost one order of magnitude, are measurable. Moreover, the initial anisotropy at time zero ($A_{0\,\mathrm{eff}} = \sum \beta_i$) does not exhibit the A_0 value measured in vitrified medium (Vincent et al. 1988), indicating the existence of even faster motions of the *Trp-59* residue in the picosecond time-scale.

The interactions with SDS micelles produce large effects on the contributions to the anisotropy decay of the measurable rotational correlation times. The initial anisotropy value reaches that observed for the apocytochrome *c* protein in vitrified medium (Vincent et al. 1988), indicating that all the rotations are resolved in the complex, in contrast to the protein in buffer solution. The contribution of the subnanosecond rotation (θ_1) is less important. The nanosecond motion (θ_2), probably reflecting the local deformation motion of the peptide chain segment where the *Trp-59* is located, is also strongly reduced. All these effects contribute to the increase in the contribution of the long correlation time. The protein therefore becomes more rigid at the SDS micelle contact. However, the short correlation time values themselves exhibit similar values to those in solution. The overall

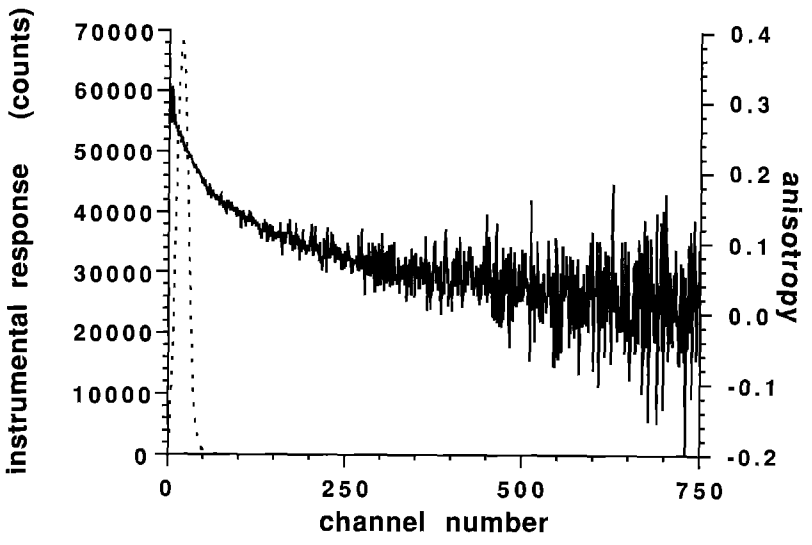

Fig. 4. Fluorescence anisotropy decay (——) of *Trp-59* of apocytochrome *c* in interaction with SDS micelles (0.5%). (. . .) Instrumental response function

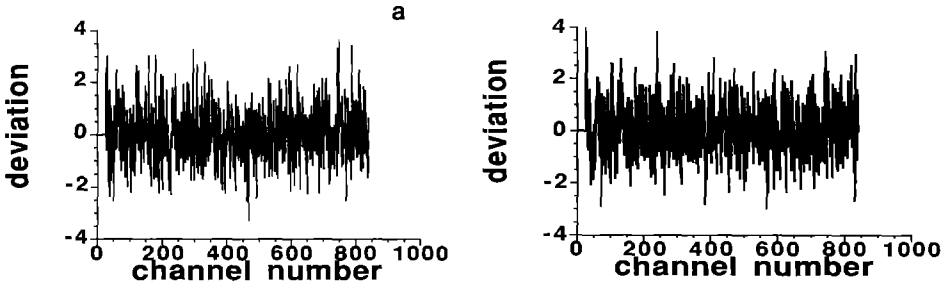

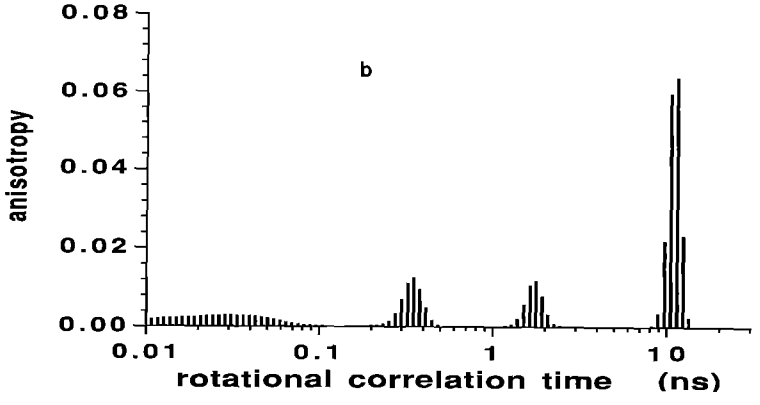

Fig. 5a, b. MEM recovered spectra of *Trp-59* rotational correlation time distribution of apocytochrome *c* in interaction with SDS micelles (0.5%) (**b**). As described in Materials and methods, a global analysis was performed on I_{vv} and I_{vh}. The deviation functions for the fit on I_{vv} and I_{vh} are presented in insert (**a**) (left and right, respectively)

Table 2. Fluorescence anisotropy decay parameters of *Trp-59* in horse heart apocytochrome *c* in aqueous solution and in interaction with surfactant micelles and POPS SUV. Apocytochrome *c* concentration: 20 μM in 0.01 M sodium phosphate buffer pH 7.04. Temperature: 20 °C. Excitation wavelength: 300 nm (band width: 5 nm). Emission wavelength: 350 nm (band width: 10 nm). Data analysis were performed with MEM as a sum of exponentials. For ω_{max} and S_1 calculations, a A_0 value of 0.295 was used (Vincent et al. 1988)

Sample	β_1	β_2	β_3	$\theta_{1(ns)}$	$\theta_{2(ns)}$	$\theta_{m(ns)}$	$A_{0\,eff}$	ω_{max} (°)	S_1
Buffer	0.091	0.103	0.070	0.29	1.79	13.6	0.264	34	0.77
SDS	0.051	0.041	0.173	0.34	1.74	10.9	0.319	27	0.85
C12PN	0.072	0.074	0.155	0.47	2.14	11.3	0.301	24	0.88
C12PG	–	0.081	0.168	–	3.07	41.0	0.249	20	0.92
C14PG	–	0.077	0.115	–	4.30	21.7	0.192	29	0.81
POPS	–	0.047	0.125	–	3.05	∞	0.172	34	0.76

Table 3. Calculation of the Stokes radii for the different apocytochrome *c*/surfactant complexes

Surfactant	R(Å)
None	23.5
SDS	21.9
C12PN	22.2
C12PG	34.1
C14PG	27.6

rotational correlation time value of the complex is decreased slightly as compared to that of the uncomplexed protein.

The dynamic state of the *Trp-59*, when the apocytochrome *c* is included in a complex with C12PN or C12PG, is significantly different from that in solution. The nanosecond flexibility (θ_2) is slowed down. A fast motion is still present and measurable in C12PN, the initial anisotropy value ($A_{0\,\mathrm{eff}}$) being equal to that measured in vitrified medium (A_0). In C12PG, the initial anisotropy value ($A_{0\,\mathrm{eff}}$) is smaller than the A_0 value. A very fast mobility is therefore likely to be effective, with a reduced amplitude (Table 2). The different sizes of the complexes formed between the protein and the surfactants are described by the long correlation time values measured on the anisotropy decays (Table 3). The complex with C12PG appears to be much larger than with the other surfactants. It should be mentioned that micelles of C10PG precipitated in the presence of the apocytochrome *c* protein, impeding any measurements on this sample.

The interaction of the apocytochrome *c* protein with vesicles of POPS reduces the contribution and the rate of the nanosecond flexibility (θ_2) (Table 2). However, a large contribution of faster motion(s) is likely to be effective since the initial anisotropy value ($A_{0\,\mathrm{eff}}$) is the lowest observed in all the samples studied. The higher mobility of the *Trp-59* residue in the complex with POPS than in the complexes with the other surfactants, is demonstrated by the large wobbling angle value which appears to be as large as that in buffer solution (Table 2). The overall correlation time of the complex cannot be measured and is represented on the analysis by an infinite value.

Discussion

The high flexibility of apocytochrome *c* in aqueous solution is further demonstrated by the anisotropy decay of *Trp-59*: fast rotational motions of the indole ring and deformation motions of the peptide chain are observed at pH 7, as they were at pH 5 (Vincent et al. 1988). However, despite this flexibility, *Trp-59* appears to be involved in discrete sets of interactions with other parts of the protein as suggested by the existence of only four discrete excited state populations. The persistence of local structure is also suggested by the ability to measure the long rotational correlation time of the protein, indicating the existence of hindrances to the internal motion of *Trp-59*.

Upon binding of the protein to organized lipid assemblies, modifications of the balance of the already existing conformational substates occur in addition to the appearance of new lifetime classes arising from interactions with the host lipid.

Two distinct types of membrane models can be separated according to their effects on the excited state lifetime distribution. In the first one (SDS), a strong increase of the contribution of the shortest excited state lifetime class is observed. In the second one, comprising the POPS vesicles and the monoalkyl PN and PG micelles, there is an increase of the contribution of the long lifetime class. The short lifetime contribution remains either constant or suppressed in POPS.

Several arguments suggest that in the SDS micelles, the *Trp-59* is located in the polar head group region of the micelle and not embedded into the alkyl chain. The reduction of the mean excited state lifetime value accompanied by an equivalent fall in the fluorescence intensity (Snel et al. 1991) can be explained by the proximity of the sulfur atom in the polar head groups of SDS, which can strongly favor non-radiative deactivation processes (Cowgill 1967; Steiner and Kirby 1969). Short range interactions between the excited state aromatic ring and the sulfur atom may occur, thereby facilitating the dissipation of the excitation energy.

The interactions of the apocytochrome *c* protein with surfactant micelles appears to be quite different from that of an integral membrane protein: the M13 coat protein (Datema et al. 1987). In the complex with SDS, this last protein did not present the above-described shift of the lifetime distribution towards short lifetime. On the contrary, there was a large contribution (50%) of a long excited state lifetime ($\sim$ 5.5 ns) as in deoxycholate micelles (Johnson and Hudson 1989). The *Trp* fluorescence emission maximum in the complex of the protein with SDS was at $\sim$ 330 nm, indicative of an apolar medium, in line with the location of the *Trp-26* in a highly hydrophobic aminoacid sequence. These data show that *Trp-26* may therefore be embedded into the surfactant alkyl chains. By contrast, the sequence of apocytochrome *c* presents a large number of polar amino acids in proximity to the *Trp-59*. In SDS, the value of the emission maximum was $\sim$ 338 nm (Rietveld et al. 1985). Similar moderate blue shifts of the *Trp* fluorescence emission maximum were observed upon incorporation of proteins such as myelin basic protein and several peptide hormones into reverse micelles of AOT in isooctane (Nicot et al. 1985; Gallay et al. 1987), despite the fact that the peptides were located in the aqueous micelle interior as shown by the accessibility of the *Trp* residue to water soluble reagents. The blue shift in the emission spectrum can therefore be due to a polarizability effect in these reverse micelles as it could also be in the present membrane systems.

All these observations strongly suggest that in SDS micelles the *Trp-59* is located close to the polar head groups and that the interactions with the polar group induces the dominant non-radiative process. Photochemically induced dynamic nuclear polarization proton NMR experiments have also indicated a localization of

the *Trp-59* residue in the interface of the SDS micelle (Snel et al. 1991).

In addition to the changes in the excited state lifetime distribution, a decrease in the barycenter values of the excited state lifetime classes was observed. This can be the result of the induction of protein secondary structure at the micelle interface with water (Rietveld et al. 1985; de Jongh and de Kruijff 1990). A more compact structure of the protein in partially α-helical form should bring the *Trp-59* indole ring closer to specific aminoacid side chains, making more efficient their quenching potencies.

In the other membrane systems, a strong contribution of the long excited state lifetime population is observed, comparable to what has been reported for the M13 coat protein (Datema et al. 1987; Peng et al. 1990). The strong contribution of this lifetime class may indicate a less polar or polarizable surrounding medium. The close similarity between temperature effects on the excited state lifetime barycenters observed in solution and in POPS vesicles strongly suggest that the *Trp-59* is not shielded from collisions with solvent molecules or protein groups when bound to the membrane bilayer. This would suggest a location of *Trp-59* at the membrane surface, where the polarizability is lower than in bulk solution. Moreover, the absence of very long excited state lifetime classes such as observed in model α-helical peptides (Vogel et al. 1988), precludes the existence of transmembrane helices of peptide segments bearing the *Trp-59* residue. This is in agreement with former data – moderate blue-shift of the emission wavelength maximum of *Trp-59*, relatively weak increase in fluorescence intensity upon interaction with PS vesicles and low efficiency of quenching by selectivity brominated phospholipids (Rietveld et al. 1985; Berkhout et al. 1987) – which suggested that *Trp-59* is not penetrating the hydrophobic region of the bilayer.

The electrostatic interactions were shown to have an important contribution of ordering the peptide chain according to recent CD measurements (de Jongh and de Kruijff 1990). A correlation appears to exist between the induction of protein secondary structure elicited by the interaction of the protein with membrane models and the excited state lifetime distribution, the higher the amount of helical structure, the higher the contribution of the short excited state lifetimes.

The correlation between secondary structure and dynamic parameters in surfactant micelles is even more evident. The strongest restriction in the *Trp* fast motion occurs for the C12PG/apocytochrome *c* complex in which the highest content of α-helical structure has been found by CD measurements (de Jongh and de Kruijff 1990). The contribution of the intermediate motion, probably reflecting the deformation motion of the peptide segment bearing the *Trp-59* residue, is reduced in the complexes. The strongest effect is observed in C14JPG micelles.

In POPS vesicles, the protein intermediate flexibility (θ_2) is reduced in rate and in amplitude. However, there is not effect on the amplitude of the fast internal rotation of *Trp-59* in the POPS/apocytochrome *c* complex as compared to the protein in solution, as suggested by the much lower $A_{0\,\mathrm{eff}}$ value than the expected A_0 one ($A_0 = 0.295$ at excitation wavelength, Vincent et al. 1988). The indole ring seems therefore to be as free to move in the complex with POPS membrane as in water solution. This suggests that the *Trp-59* region is not located in a α-helix.

In conclusion, we have found large modifications of the dynamics of apocytochrome *c* in different time scales when the protein is transferred from water to a membrane interface. The conformational equilibrium between local substates of the protein, corresponding to a slow process in the fluorescence time scale is modified, as well as faster processes such as internal rotation of the indole ring and segmental flexibilities. There is a correlation between the induction of ordered secondary structure of the protein and its internal dynamics: a high content of α-helical structure corresponds to a restricted fast internal motion but the segmental flexibilities which are reduced in rate, are still of large amplitude. It appears from the different parameters that at least the *Trp-59* does not penetrate into the lipid alkyl chain but rather stays at the membrane or the micelle interface. Direct interactions with the SDS polar head groups is demonstrated. The interaction between apocytochrome *c* and POPS systems appears to preserve the fast dynamics of the indole ring. A location at the membrane surface of the part of the protein bearing the *Trp-59* is compatible with the reduction of the fast phospholipid motion and the large disorganization of the lipid acyl chain (Jordi et al. 1990).

Acknowledgements. The technical staff of LURE is acknowledged for running the synchrotron machine during the beam session. W. Jordi, H. H. M. de Jongh and B. de Kruijff are gratefully acknowledged for their gift of the protein and surfactants. We wish to thank J. C. Brochon for providing us with the program for the analysis of the rotational correlation time distribution by the Maximum Entropy Method. This work was partially granted by INSERM (CRE 879015).

References

Berkhout TA, Rietveld A, De Kruijff B (1987) Preferential lipid association and mode of penetration of apocytochrome *c* in mixed model membranes as monitored by tryptophanyl quenching using brominated phospholipids. Biochim Biophys Acta 897:1–4

Brochon JC, Livesey AK (1991) (in preparation)

Brochon JC, Livesey AK (1987) Time-resolved fluorimetry using synchrotron radiation and Maximum Entropy Method of analysis. In: Douglas RH, Moan J, Dall'Acqua F (eds): Proceedings of the 2nd Congress of the European Society for Photobiology. Plenum Press, New York, pp 21–29

Chang MC, Petrich JW, McDonald, DB, Fleming GR (1983) Non-exponential fluorescence decay of tryptophan, tryptophylglycine and glycyltryptophan. J Am Chem Soc 105:3819–3824

Cowgill RW (1967) Fluorescence and protein structure. XI-Fluorescence quenching by disulfide and sulhydryl groups. Biochim Biophys Acta 140:37–44

Creed D (1984) The photophysics and photochemistry of the near-absorbing amino acids-I. Tryptophan and its simple derivatives. Photochem Photobiol 39:537–562

Datema KP, Visser AJWG, van Hoek A, Wolfs CJAM, Spruijt RB, Hemminga MA (1987) Time-resolved tryptophan fluorescence anisotropy investigation of bacteriophage M13 coat protein in micelles and in mixed bilayers. Biochemistry 26:6145–6152

De Jongh HHJ, de Kruijff B (1990) The conformational changes of apocytochrome *c* upon binding to phospholipid vesicles and micelles of phospholipid based detergents: a circular dichroism study. Biochim Biophys Acta 1029:105–112

Gallay J, Vincent M, Nicot C, Waks M (1987) Conformational aspects and rotational dynamics of synthetic adrenocorticotropin-(1-24) and glucagon in reverse micelles. Biochemistry 26:5738–5747

Hennig B, Koehler H, Neupert W (1983) in *Mitochondria.* In: Schweyen RJ, Wolff K, Kaudewitz F (eds) de Gruyter, Berlin, pp 551–561

Ichiye T, Karplus M (1983) Fluorescence depolarization of tryptophan residues in proteins: a molecular dynamics study. Biochemistry 22:2884–2893

John E, Jähnig F (1988) Dynamics of melittin in water and membranes as determined by fluorescence anisotropy decay. Biophys J 54:817–827

Johnson ID, Hudson B (1989) Environmental modulation of M_{13} coat protein tryptophan fluorescence dynamics. Biochemistry 28:6392–6400

Jordi W, de Kroon AIPM, Killian JA, de Kruijff B (1990) The mitochondrial precursor protein apocytochrome *c* influences the order of the headgroup and acyl chain of phosphatidylserine dispersions. A ^2H and ^{31}P NMR study. Biochemistry 29:2312–2321

Kinosita K, Kawato S, Ikegami A (1977) A theory of fluorescence polarization decay in membranes. Biophys J 20:289–305

Kuipers OP, Vincent M, Brochon JC, Verheij HM, de Haas GH, Gallay J (1990) Effects of ligand binding on the conformation and internal dynamics in specific regions of porcine pancreatic phospholipase A_2 with tryptophan as probe: a study combining time-resolved fluorescence spectroscopy and site-directed mutagenesis. Proc Soc Opt Eng 1204:100–111

Levy RM, Szabo A (1982) Initial fluorescence depolarization in tyrosines in proteins. J Am Chem Soc 104:2073–2075

Lipari G, Szabo A (1980) Effect of librational motion on fluorescence depolarization and nuclear magnetic relaxation in macromolecules and membranes. Biophys J 30:489–506

Livesey AK, Brochon JC (1987) Analyzing the distribution of decay constants in pulse-fluorimetry using the Maximum Entropy Method. Biophys J 52:693–706

Nicot N, Vacher M, Vincent M, Gallay J, Waks M (1985) Membrane protein in reverse micelles: Myelin basic protein in a membrane-mimetic environment. Biochemistry 26:5739–5747

Peng K, Visser AJWG, van Hoek A, Wolfs CJAM, Hemminga MA (1990) Analysis of time-resolved fluorescence anisotropy in lipid-protein systems. II Application to tryptophan fluorescence of bacteriophage M13 coat protein incorporated in phospholipid bilayers. Eur Biophys J 18:285–293

Petrich JW, Chang MC, McDonald DB, Fleming GR (1983) On the origin of nonexponential fluorescence decay in tryptophan and its derivatives. J Am Chem Soc 105:3824–3832

Rietveld A, Ponjee GAE, Schiffers P, Jordi W, Van de Coolwick PJFM, Demel RA, Marsh D, De Kruijff B (1985) Investigations on the insertion of the mitochondrial precursor protein apocytochrome *c* into model membranes. Biochim Biophys Acta 818:398–409

Snel MME, Kaptein R, de Kruijff B (1991) Interaction of apocytochrome *c* and derived polypeptide fragments with sodium dodecyl sulfate micelles monitored by photochemically induced dynamic nuclear polarization H^1 NMR and fluorescence spectroscopy. Biochemistry 30:3387–3395

Steiner RF, Kirby EP (1969) The interaction of the ground and excited states of indole derivatives with electron scavengers. J Phys Chem 73:4130–4135

Szabo AG, Rayner DM (1980) Fluorescence decay of tryptophan conformers in aqueous solution. J Am Chem Soc 102:554–563

Vincent M, Brochon JC, Merola F, Jordi W, Gallay J (1988) Nanosecond dynamics of horse heart apocytochrome *c* in aqueous solution as studied by time-resolved fluorescence of the single tryptophan residue (*Trp-59*). Biochemistry 27:8752–8761

Vogel H, Nilsson L, Rigler R, Voges KP, Jung G (1988) Structural fluctuations of a helical polypeptide traversing a lipid bilayer. Proc Natl Acad Sci USA 85:5067–5071

Wahl Ph (1979) Analysis of fluorescence anisotropy decay by least square method. Biophys Chem 10:91–104